ELSEVIER

Cement & Concrete Composites 26 (2004) 31–39

Cement & Concrete Composites

www.elsevier.com/locate/cemconcomp

Influence of silica fume addition on concretes physical properties and on corrosion behaviour of reinforcement bars

J.M.R. Dotto [a], A.G. de Abreu [b], D.C.C. Dal Molin [b], I.L. Müller [c,*]

[a] Department of Structures and Civil Construction, Federal University of Santa Maria, 97119-900 RS, Brazil
[b] Department of Civil Engineering, Federal University of Rio, Grande do Sul, Av. Osvaldo Aranha, 99-90035-190 Porto Alegre, RS, Brazil
[c] Department of Metallurgy, Federal University of Rio, Grande do Sul, Av. Osvaldo Aranha, 99-90035-190 Porto Alegre, RS, Brazil

Abstract

The addition of silica fume (SF) in concretes has been proposed as a form to improve their performance in resisting concrete reinforcement corrosion. In this study an experimental program on compressive strength, porosity, electrical resistivity and polarization curves was carried out with the purpose of evaluating the effect of different SF additions (0%, 6% and 12%). Concretes with different water–binder ratio (cement + SF) 0.50, 0.65 and 0.80 were used. The results have allowed to show that there are significant improvements of the concrete properties with the SF addition, suggesting its use in aggressive environments.

Keywords: Concrete durability; Silica fume; Corrosion; Corrosion potential; Electrical resistivity; Polarization curves

1. Introduction

The addition of silica fume (SF) has proved to improve both the compressive strength and durability of concrete. Also, the presence of this admixture has been shown effective in increasing the electrical resistivity [1] and the durability of concrete exposed to aggressive conditions like chloride containing environments [2].

Pozzolanic materials are generally able to combine with the hydrated calcium hydroxide ($Ca(OH)_2$) forming the hydrated calcium silicate (C–S–H), which is the principal responsible for the strength of hydrated cement pastes. Also, an increase in the bulk density of concrete results as the mixture voids are filled with very small admixture particles (*micro filler effect*) [3]. The SF can produce both chemical and physical effects, which cause meaningful changes in the microstructure of concrete, diminishing its permeability and improving its strength [4].

It has been shown [5] that the physical effect of SF, at 7 days, has an influence on compressive strength. At 28 days, both chemical and physical effects are significant. A scanning electron microscope (SEM) analysis of 16 years old concrete with addition of SF shows that the microstructure of this material is more homogeneous and dense than the concrete without SF [6]. The high porosity of the matrix of the concrete without addition of SF explains its lower strength and higher permeability to chloride ions.

The most important region in the microstructure of the concrete is around the aggregate. The addition of SF in concrete leads to reduction in porosity of the transition zone between matrix and aggregate in the fresh concrete and provides the microstructure needed for a strong transition zone [7]. Investigation on the aggregate-matrix interface concluded that, in concrete with SF, a transgranular fracture is observed, hence, the cracks usually traversed the aggregates, pointing to a lower porosity of the interfacial zone as a result of SF inclusion [8].

This overview shows the development of research about physical properties of concrete with SF addition, but the corrosion behaviour of reinforcement steel and electrical properties of concrete are also important for the sake of increased durability. The present paper investigates some of the parameters that have important influences on the corrosion process of the steel reinforcement embedded in concrete. The porosity, the

* Corresponding author. Tel.: +55-51-3316-3573; fax: +55-51-3316-3988.
E-mail addresses: ilmuller@vortex.ufrgs.br, ilmuller@vortex.ufrgs.dr (I.L. Müller).

0958-9465/$ - see front matter © 2003 Elsevier Ltd. All rights reserved.
doi:10.1016/S0958-9465(02)00120-8

Table 1
Physical characteristics (Panel A) and chemical analysis (Panel B) of high portland cement and SF

	Cement	SF						
Panel A: Physical characteristics								
Compressive strength, 5 × 10 cylinder (MPa)								
3 days	36.7	–						
7 days	42.3	–						
28 days	47.7	–						
Setting time (initial, min)	125	–						
Fineness #0.075 mm (%)	0.8	–						
Fineness #0.045 mm (%)	0.5	7.0						
Specific gravity (g/cm^3)	3.12	2.22						
BET specific surface area (m^2/g)	1.22	13.86						
Means size (μm)	–	0.50						
Pozzolanic activity index (%)								
Water requirement	–	133						
Activity index (28 days)	–	91						
Panel B: Chemical analysis								
Oxides (%)	SiO_2	CaO	Fe_2O_3	Al_2O_3	MgO	SO_3	Na_2O	K_2O
Cement	19.679	64.02	2.62	5.01	1.38	3.11	0.03	0.84
SF	90.21	0.30	0.15	0.12	0.73	0.01	0.46	1.51

electrical resistivity and the corrosion behaviour of steel in concretes with and without SF were evaluated with the objective to verify the effectiveness of this addition for use in aggressive environments.

2. Experimental

2.1. Concrete materials and parameters

A high early strength portland cement [1] available in the Brazilian market and SF from the production of a silicon metal industry were used. Physical characteristics and chemical analysis of these materials are shown in Table 1 (Panel A and B).

The coarse aggregate was basalt and the fine aggregate was taken from the Guaiba River (Porto Alegre, Brazil). The physical characteristics of these aggregates are shown on Table 2.

The variables tested were the water–binder ratio ($w/(c + SF) = 0.50$, 0.65 and 0.80) and the content of SF by weight of cement (0%, 6% and 12%). The concrete mixture proportions used, workability (by slump test) [10] and compressive strength [11] are shown in Table 3. The compressive strength measurements were done in triplicate on cylindrical test specimens ($\varnothing 10 \times 20$ cm) for each concrete mixture.

[1] Type CP-V according to Brazilian standard—NBR5733, equivalent to the ASTM C 150 Type III [9].

2.2. Test methods

For the determination of porosity, three 170 × 100 × 100 mm prismatic specimens were cast for each concrete mixture. The concrete was cured for 28 days and at the age of 91 days, the specimens were oven dried at 105 °C to constant weight prior to the test. After that, the specimens were immersed in potable water for 72 h at room temperature and then they were immersed in boiling water for 5 h. Porosity was calculated by measuring dry, saturated and buoyant weights of the specimens.

The reactivity of the SF was evaluated using an accelerated test: stipulated proportions of high portland cement (65%) and SF (35%) were mixed with sand, and water was added to give a flow of (225 ± 5)mm, measured with the help of a flow table. X-ray diffraction (Siemens Difractometer—Diffrac 500, CuKα, 2°/min) was used to evaluate qualitatively the calcium hydroxide (portlandite) consumption.

The electrical resistivity of concretes was determined by the Wenner method (four points method), adapted from ASTM G 57 [12], with the specimens immersed in potable water. Details of the procedure are given in

Table 2
Characteristics of coarse and fine aggregates

Characteristic	Coarse aggregate	Fine aggregate
Fineness modulus	6.95	2.66
Maximum size (mm)	25	4.80
Form index	3.36	–
Specific gravity (g/cm^3)	2.77	2.61

Table 3
Mixture proportions and correspondent mean compressive strength at 28 days

Mix no.	Water–binder ratio	Materials (Kg/m^3)					Slump (mm)[a]	Compressive strength (MPa)[b]
		Cement	SF	Fine aggregate	Coarse aggregate	Water		
1	0.50	375	–	637	1189	187	78	42.3
2		367	22	624	1163	194	75	51.2
3		359	43	624	1163	201	78	56.1
4	0.65	286	–	721	1181	186	105	26.6
5		281	17	708	1160	194	98	35.1
6		275	33	693	1160	200	81	36.5
7	0.80	232	–	772	1178	186	83	19.5
8		228	14	759	1158	193	105	27.7
9		224	27	746	1138	200	92	29.7

[a] According to the ASTM C143/C143M [10].
[b] According to ASTM 39 [11].

reference [13]. The specimens for these measurements are shown in Fig. 1a. The measurements were done when the specimens were at the age of 98, 112 and 217 days. The results were averaged over four specimens for each concrete mixture.

For electrochemical essays on steel in concrete, e.g. plotting of polarization curves and corrosion potential (E_{corr}) measurements, cylindrical test specimens which size and characteristics are shown in Fig. 1b were used. A graphite rod embedded in the concrete was used as counter electrode and a saturated calomel electrode (SCE) as reference electrode. The essays were performed 9 months after the casting of the specimens. During this time, the specimens were maintained on controlled conditions (23 °C, RH 80–90%) and then exposed to the laboratory air for 7 days before the tests. Anodic and cathodic polarization curves for the steel embedded in concrete were performed with the potentiostatic method, the potential being changed in steps of 10 mV each minute, starting from the corrosion potential. The equipment used was a Wenking potentiostat model ST 72. The ohmic drop (IR drop) between reference and working electrodes was evaluated through the current interruption technique and the potential decay was recorded with a Tektronix oscilloscope model TDS 320. These values were used to correct the polarization curve for IR drop.

The corrosion potential (E_{corr}) of the steel in concrete was determined according to the procedure described in ASTM C 876 [14], with the same type of specimens of Fig. 1b, beginning nine months after their casting as well. After that time, in order to accelerate the corrosion process, the cylindrical specimens were subjected to a cyclic treatment with 2 days partial immersion in a 3. 5% NaCl solution and 5 days drying in air, during 350 days. E_{corr} was measured at the beginning and at the end of each wet/dry cycle using a SCE and a high-input impedance voltmeter. After the test period was over, the steel specimens were pulled out from the concrete. Visual observation data of corrosion in terms of percentage of rusted area were recorded.

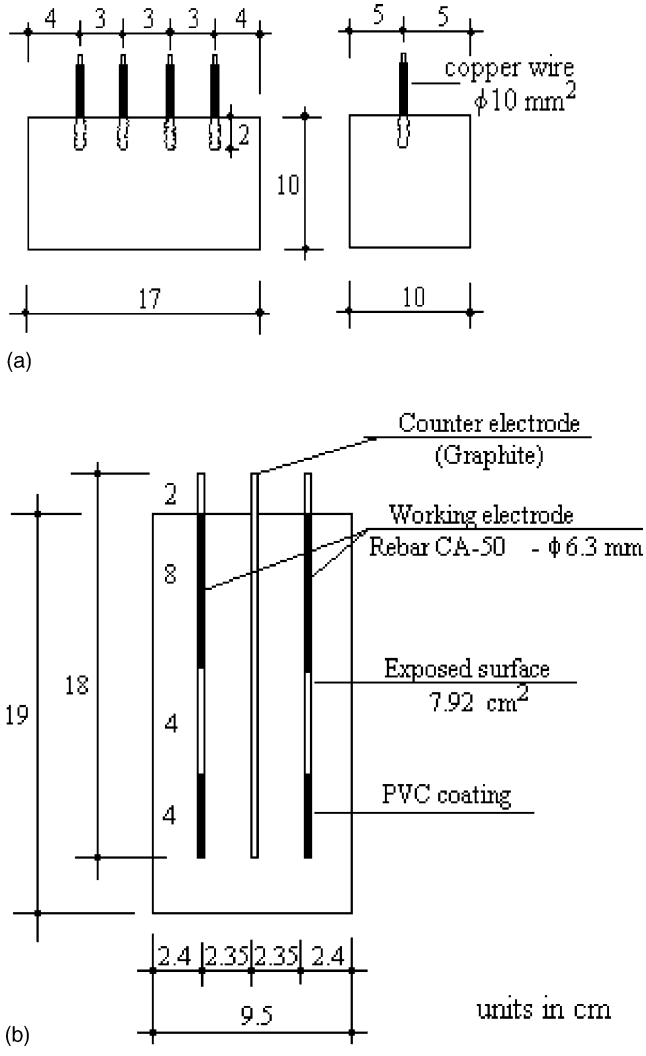

Fig. 1. Schematic illustration of the concrete specimens for: (a) electrical resistivity measurements, (b) polarization curves and corrosion potential measurements.

The electrochemical behaviour of bare steel was determined by plotting polarization curves in three simulated concrete pore solutions. They were prepared mixing 100 g of plain cement or 100 g of binder (88% of high portland cement and 12% of SF) in one liter of distilled water. In one case, to simulate the pore fluid of a chloride-contaminated concrete, NaCl was added to the SF containing solution in a concentration of 0.3%. After 24 h the liquid was filtered and used immediately. The working electrode consisted of the lateral area of a cylindrical steel bar (1.0 cm^2) which was cleaned with inhibited hydrochloric acid solution and degreased with acetone. It was then immersed in a cell containing the simulated concrete pore solution for 60 min before E_{corr} was measured and the polarization curve was run. A SCE was used as reference electrode and a platinum wire as counter electrode.

3. Results and discussions

3.1. Physical tests

Table 3 presents the mean compressive strength at 28 days for all mixtures studied. A comparison of the resistivity data (Fig. 2) and the compressive strength data suggests the presence of an direct relationship between them, as to be expected. The higher the resistivity the higher the compressive strength. Tests by Whittington et al. [15] found that the values of resistivity and the water/cement ratio are inversely proportional, i.e. as the strength increase, the resistivity increase.

Both 6% and 12%SF concrete mixtures showed a gain in compressive strengths compared with the plain concrete and the last one showing a slightly higher gain than the concrete containing 6%SF. SF provides additional improvement to the porosity and hence the pore structure of concrete. This is reflected in the improved strength and transport properties [16]. The SF positively modifies the interfacial transition zone microstructure [17] that, in turn, contributes positively to reduce the electrical conductance of the system.

The results presented in Table 4, show that an increase in water–binder ratio increases the porosity values, probably due to the larger capillary pores being altered. However, the SF addition has a negligible effect on porosity contrary to what is claimed by other authors [16]. This result is probably due to the fact that SF produces a refinement of pore structure [18], without further reduction in total porosity [7]. The porosity measurements adopted in this study determines the total pore volume gravimetrically, and the values are higher than the ones measured by either mercury intrusion porosimetry (MIP) or nitrogen desorption [19]. The access of both the anodic (Cl^-) and cathodic agents (e.g. O_2), which cause reinforcement steel corrosion, may be easier in higher porosity concretes.

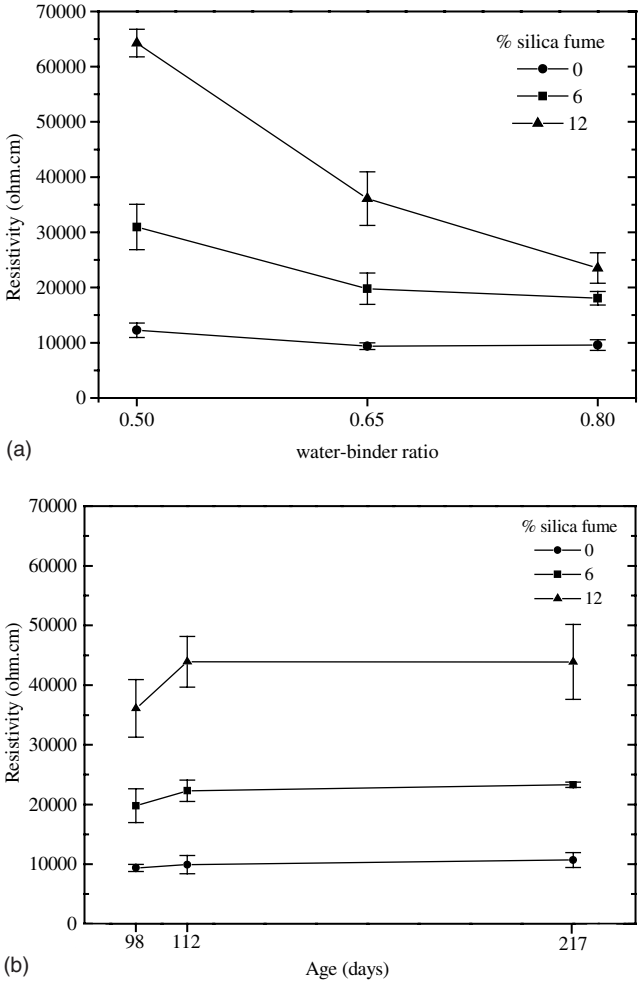

Fig. 2. Effect of SF addition on the electrical resistivity of concretes: (a) relation between the electrical resistivity and water–binder ratio for different SF contents, at 98 days, (b) relation between the mean values of the electrical resistivity and age for different SF content, for a water–binder ratio of 0.65.

Table 4
Mean porosity of concretes of different water–binder ratio at age of 91 days

%SF	Water–binder ratio		
	0.50	0.65	0.80
0	11.93a	14.04b	14.23b
6	11.20a	13.96b	14.32b
12	12.40a	12.38a	14.39b

* Values followed by the same letter do not present statistically significant difference (Duncan test).

Furthermore, the concrete electrical resistivity increases with the increasing amount of SF, as represented in Fig. 2. When compared to the reference concrete, the addition of 12% of SF increased the resistivity up to 5.2,

3.85 and 2.45 times, for the water–binder ratios of 0.50, 0.65 and 0.80, respectively. The coefficients of variation were less than 13.2%, 14.3% and 11.7% for the water–binder ratios 0.50, 0.65 and 0.80 with and without SF addition, respectively. To statistically prove the influence of the investigated variables on the electrical resistivity, as well as to verify the existence of significant interactions between variables, an analysis of variance was performed. This approach allows the comparison of different groups of observations through the comparison of the variance observed between groups with the variance observed into each group, for a specific level of significance. The analysis of the electrical resistivity variance is summarised in Table 5, for a 5% level of significance.

According to Table 5, the SF content was the most important factor on the resistivity values, followed by water–binder ratio and SF content x water–binder ratio interaction, respectively. The age is insignificant for resistivity of the total period of exposure studied (119 days).

Cao et al. [20] reported results similar to those obtained in the present work for high strength concrete (70 MPa) immersed in lime-saturated water. The replacement of cement by 10% of SF increased by 1.5 times the resistivity at the age of 90 days. This behaviour was attributed to the dense microstructure of the concrete, resulting in decreasing of corrosion due to the increasing resistivity. Pore structure measurements carried out by Matte et al. [21], using MIP, showed that the porosity of the cement paste was between 0.01 and 0.02 μm and for the cement paste containing SF it was below 0.0036 μm (pores less than 36 Å cannot be measured by MIP). Hence, the high resistivity of the SF-containing concrete in the present work, can be related to the dense microstructure, which hinders the flow of ions in the concrete. The fact that the concrete porosity data did not show a strong dependence on the SF content as pointed out above must be assigned to the nature of the test method, which only determines the total porosity in terms of weight loss, but does not assess the distribution of pore size.

Diffractograms presented in Fig. 3, show the consumption of calcium hydroxide in mortars with addition of SF as a consequence of the pozzolanic reaction. Some researchers have found that the reduction of calcium

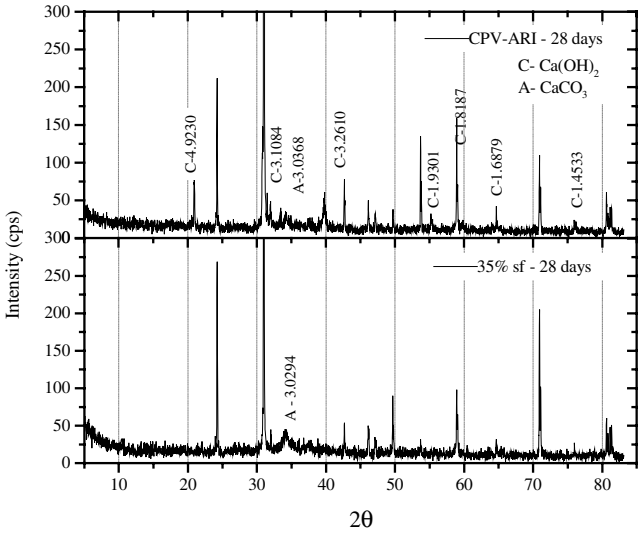

Fig. 3. X-ray spectrum of mortars with sand–cement ratios of 3:1 with: (a) portland cement (100%); (b) portland cement with replacement of 35% SF.

hydroxide is higher with increasing SF addition and age of the concrete [22]. Yogendran et al. [23] found that for a high water–binder ratio, 20% SF were required to consume all the calcium hydroxide. At a lower water–binder ratio, 15% of SF was sufficient. However, the alkalinity is not only dependent on Ca^{2+} ions, but also on the alkali content in the pore solution. Larbi et al. [24] found a decrease of the alkali content in the SF mixtures, after the first day of hydration. This decrease can be due to the absorption of Na^+ and K^+ ions by silanol groups to form alkali-rich silicates. The results in the literature are in agreement with the present data which indicate that the consumption of $Ca(OH)_2$, increases in SF-containing concrete, probably affecting the pH value in the pore solution. In fact, in the present work the simulated pore solution of concrete containing SF showed a pH roughly half an unit lower than the corresponding solution of plain concrete.

3.2. Electrochemical measurements

To obtain the polarization curves of steel embedded in concrete, determination of ohmic drop between working and reference electrodes was necessary. The

Table 5
Analysis of variance of the significant factors on resistivity measurements at 98, 112 and 217 days for concrete specimens immersed in potable water

Source of variation	Degrees of freedom	Mean square	Computed F	$F_{0.05}$
%SF	2	112440×10^5	397.75*	3.12
w/(c + SF)	2	405346×10^4	143.398*	3.12
Age	2	76812×10^2	2.69	3.12
% SF x w/(c + SF)	4	127301×10^4	45.03*	2.50
Error	80	282686×10^2		

* Significant; $F_{0.05}$—table value (Fisher distribution), level of 5% significance.

results of IR drop measurements were found to be consistently higher with the increase in SF content and decreased slightly with the increase in the water–binder ratio. For the three water–binder ratios studied, the equivalent resistance associated to the ohmic drop between reference and working electrodes was 575, 1600 and 2150 Ω for 0%, 6% and 12% SF content, respectively. This result is in accord with the higher resistivity of the SF-containing concretes reported above and may be associated to the fine porosity of the SF-containing concretes, agreeing with other similar results found in the literature [25].

Some typical anodic and cathodic polarization curves of steel embedded in concrete containing 6% SF with different water–binder ratios (Fig. 4) and with different SF content (Fig. 5) are presented. For all these tests the concretes had not been exposed to any contamination. Thus, the results represent the electrochemical behaviour of steel embedded in different concretes, at the age of 9 months, at room temperature and a RH of 80–90%. In the absence of any active corrosion, the anodic polarization curves show a typical passive zone (current density in the range of 0.1–1 μA/cm^2) followed by the oxygen evolution reaction.

The cathodic currents should correspond to the dissolved oxygen reduction reaction, since the potential has not been driven until the hydrogen evolution zone. The cathodic current density could be expected to increase with the increase in water–binder ratio, or to decrease for the higher SF contents, as a consequence of the higher permeability associated with the larger capillary pores [26] and with the porosity in the interfacial zone [27] in cementitious materials. It is known that the corrosion rate is generally limited by the rate of diffusion of oxygen, specially in water saturated concrete when for instance E_{corr} drops to potentials less than −400 mVSCE (due to steel depassivation promoted by chloride contamination or by concrete carbonation). An oxygen diffusion coefficient of 0.68×10^{-8} m^2 s^{-1} for a concrete made with ordinary Portland cement and a water–cement ratio of 0.60 has been determined by Kobayashi and Shuttoh [28]. According to Raupach et al. [29] oxygen diffusion is not a decisive factor influencing the corrosion ratio of reinforcing bars directly if oxygen diffusion coefficient for concrete is higher that 10^{-10} m^2 s^{-1}. Accordingly, in the present work, no clear trend could be found in the cathodic polarization curves for the different concretes, such as to corroborate some influence of their different porosity on the cathodic reaction.

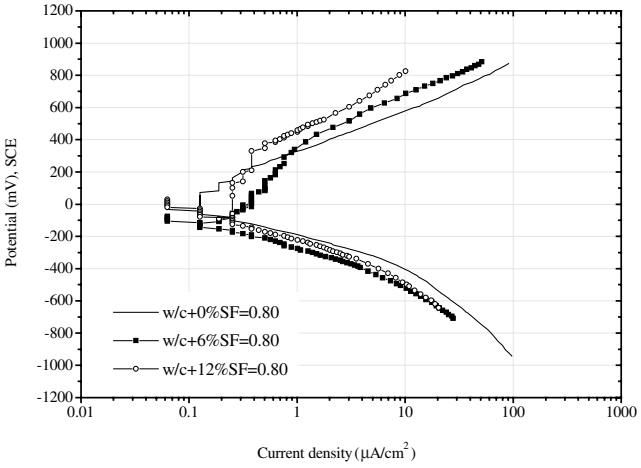

Fig. 5. Anodic and cathodic polarization curves of reinforcing steel embedded in concrete with addition of SF (0%, 6% and 12%) for a water–binder ratio of 0.80.

In Fig. 6 the polarization curves for bare steel in the simulated pore solutions of plain concrete and of SF-containing concretes, with and without addition of chloride, are to be found. E_{corr} values in this case, were more negative (−300 and −500 mVSCE) when compared

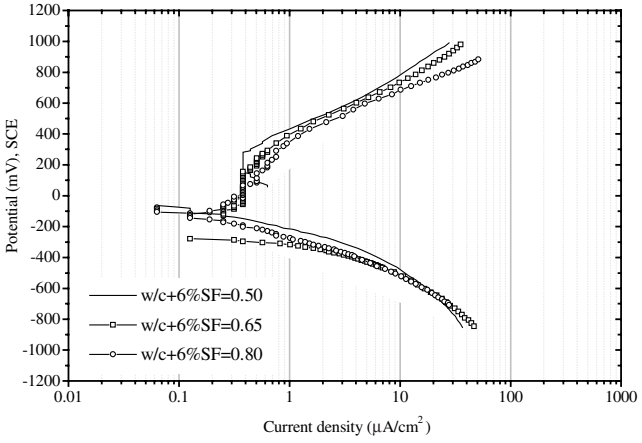

Fig. 4. Anodic and cathodic polarization curves of reinforcing steel embedded in concrete with addition of 6% SF for different water–binder ratios.

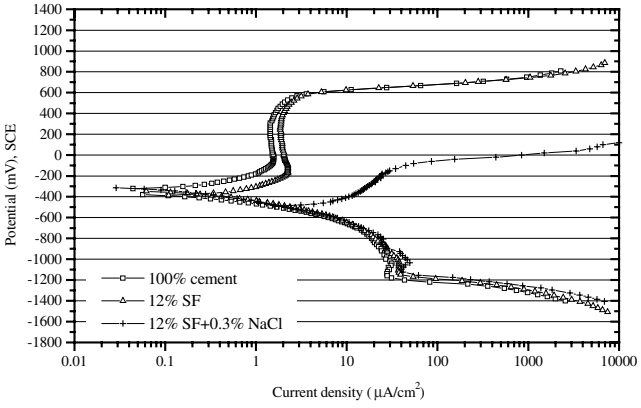

Fig. 6. Anodic and cathodic polarization curves of steel in simulated pore solution of plain concrete and of SF containing concrete, with and without 0.3% of NaCl.

with those ones of the steel bar in concrete, when these values were between +0 and −300 mVSCE, at 9 months age (Figs. 4 and 5), what is to be associated to the anodic current densities being higher, when compared with those for steel embedded in concrete. This result can be attributed to the small immersion time in the solution before the test, which in this experiment was of 60 min. It is well known that passive oxide films on iron keep growing very slowly over long periods of time, resulting in progressively lower passive current densities. Besides that, the current distribution on the steel electrode are quite different in the electrolytic cell solution and in the concrete specimen. On the other hand, the transport properties of concretes are a function of the pore size distribution, pore conductance (pore shape factor), tortuosity and isotropy [30] and mineral admixtures of the cement paste [31] differently as in the present simulated solutions.

However, Fig. 6 indicates that SF promotes an increase in passive current density values. In fact, the plain concrete pore solution (pH = 13) produces a lower current density than the SF-added concrete solution (pH = 12.5), which may be due to a decrease in alkalinity. Moreover, as can be seen on the same figure, chloride ions also contribute to increase current density in the passive zone. According to Amaral and Müller [32], passive current density values of iron in alkaline solutions are a complex function of pH, solution composition and time. On the other hand, in presence of chloride the polarization curve shows a pitting potential which is not present in the other electrolytes. However, this critical potential is quite distant from E_{corr} in that solution. Thus, the well known influence of chloride ions on the corrosion of steel in concrete should be explained by a crevice corrosion mechanism, which could be responsible for bringing down the critical potential for localized corrosion, as suggested by Sagüés et al. [33]. The slow installation of crevice corrosioen on reinforcing bars in concrete, could also explain the lowering of the E_{corr} with time as will be shown by the next results.

Results for a typical E_{corr} monitoring are shown in Fig. 7. The values tend to decrease with time for all concretes. From cycle to cycle, potential is always more negative in concretes with higher water–binder ratio. Similar behaviour was also pointed out by other researchers [34].

For the lowest water–binder ratio (0.50) no important differences were observed between the E_{corr} values of the concrete with and without SF addition. Potential did not descend to values lower than −270 mV after 350 days, indicating that in no one of the materials, steel corrosion had begun. Hou and Chung [35], have also not found depassivation of the metal in concrete with 15% of SF and water–cement ratio of 0.50, immersed in chloride environment for 25 weeks. However, the chloride environment caused the E_{corr} of rebar in plain concrete to decrease to −370 mVSCE, initially and decreasing with time. Other authors [36] have found that the E_{corr} of steel in plain concrete (w/c = 0.50) crossed the threshold potential of −270 mVSCE after 80 days of exposure to a chloride and sulfate solution and for a 10%SF concrete (w/c = 0.50) a time of 548 days was required.

For intermediate and high water–binder ratios (0.65 and 0.80), the control concrete assumed E_{corr} values definitely lower than −270 mV much earlier than the SF-containing ones. Concrete with 15%SF has been shown to decrease water absorptivity [35] and the use of SF also contributes to the refinement of the pore structure (transformation of the system containing large pores into one with smaller pores) [2] and grain refinement (transformation of large crystal, such as calcium hydroxide, into smaller crystals) was confirmed by atomic force microscopy by Papadakis et al. [19]. So, the SF can retard deterioration phenomena and elongate construction service lifetime. Visual inspection at the end of the

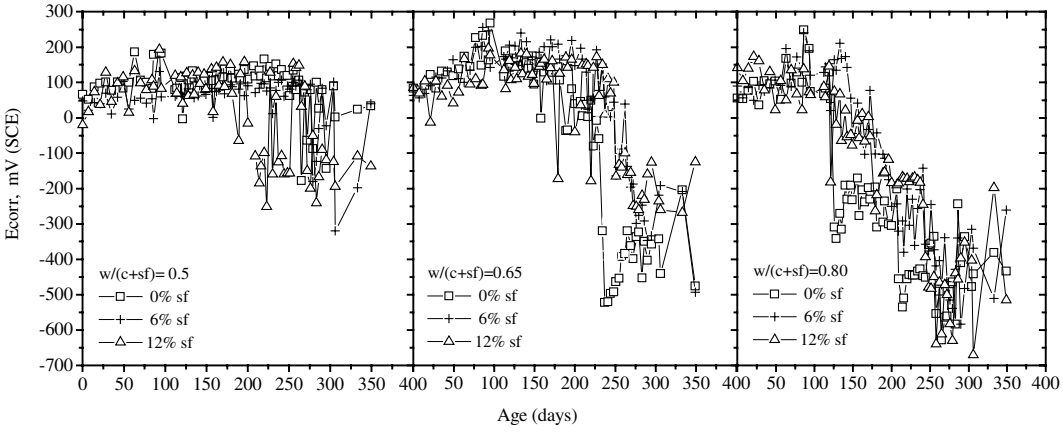

Fig. 7. Corrosion potential of the reinforcing steel bar in concrete subjected to drying (5 days) and wetting (2 days) cycles in 3.5% NaCl solution.

cyclic treatment confirmed that steel in concrete with 0.80 water–binder ratio without SF was heavily corroded over the whole exposed area (~90%), whereas, the specimens containing SF showed only a slight corrosion on some 25% of the steel area. Hence, the present results indicate that, at least for the concretes with 0.65 and 0.80 water–binder ratios, SF hinders the entrance and the depassivating effect of chloride, delaying the onset of corrosion. This must be related with the above cited influence of this admixtures on the porosity and water absorptivity of the concrete.

4. Conclusions

- The results obtained show that the addition of 6% of SF increases the electrical resistivity of concrete by 2.5 times and 12% of SF increases it by 5 times. This suggests that the addition of SF can be effectively used in protecting steel reinforcement against corrosion.
- Based on X-ray diffraction results, the addition of silica fume is expected to reduce the pH of the concrete pore solution (mainly because of the portlandite consume). An increase in passive current of steel is correspondingly found in SF containing aqueous solution simulating concrete pore solution. However, the improved electrical resistivity and dense microstructure of concrete yielded by the addition of SF, are expected to be efficient on protecting steel reinforcement from corrosion in concrete.
- The time to corrosion onset of reinforcement steel in concrete contaminated by chloride is greater in SF-containing concretes than in plain concrete specimens. This time seems to be more dependent on the physical characteristics (porosity, resistivity, addition) than on the chemistry of the concrete pore solution.

References

[1] Abreu AG, Dal Molin DCC. Effect of silica fume addition on electric resistivity of normal strength concrete. In: IV Congresso Iberoamericano de Patologia das Construções, VI Congresso de Controle de Qualidade, Anais, vol. 1. LEME/CPGEC, Dpto. de Eng. Civil, Universidade Federal do Rio Grande do Sul, Porto Alegre. 1997. p. 201–8 [in Portuguese].

[2] Delagrave A, Pigeon M, Marchand J, Revertégat E. Influence of chloride ions and pH level on the durability of high performance cement pastes (part II). Cement Concr Res 1996;26(5):749–60.

[3] Wolf J. Study about durability of high-performance concrete with silica fume addition. Master in Engineering thesis. P. Alegre, Engineering School of Universidade Federal do Rio Grande do Sul, 1991 [in Portuguese].

[4] Isaia GC. Effects of binary and ternary pozzolanic mixtures in high portland concrete: a durability study, PhD thesis. S. Paulo, Polytechnic School of Universidade de São Paulo, 1995 [in Portuguese].

[5] Detwiler RJ, Mehta PK. Chemical and physical effects of silica fume on the mechanical behavior of concrete. ACI Mater J 1989;86(6):609–14.

[6] Lachemi M, Tagnit-Hamou AE, Aïtcin C. Long-term performance of silica fume concretes. Concr Int 1998;20(1):59–65.

[7] Goldman A, Bentur A. Bond effects in high-strength silica-fume concretes. ACI Mater J 1989;86(5):440–7.

[8] Tasdemir C, Tasdemir MA, Lydon FD, Barr BIG. Effects of silica fume and aggregate size on the brittleness of concrete. Cement Concr Res 1996;26(1):63–8.

[9] ASTM C 150. Standard specification for Portland cement. Philadelphia: American Society for Testing and Materials. 1997.

[10] ASTM C 143/C 143 M. Test method for slump of hydraulic cement concrete. Philadelphia; American Society for Testing and Materials. 1998.

[11] ASTM C 39. Standard test method for compressive strength of cylindrical concrete specimens. Philadelphia; American Society for Testing and Materials. 1996.

[12] ASTM G 57. Standard method for field measurement of soil resistivity using the Wenner four-electrode method. American Society for Testing and Materials. Philadelphia, 1984.

[13] Abreu AG. Effect of mineral admixtures on electric resistivity of normal strength concretes. Master in Engineering thesis. P. Alegre, Engineering School of Universidade Federal do Rio Grande do Sul, 1998. (in Portuguese).

[14] ASTM C 876. Standard test for half-cell potentials of uncoated reinforcing steel in concrete. American Society for Testing and Materials. Philadelphia, 1991.

[15] Whittington HW, McCarter J, Force MC. The conduction of electricity through concrete. Mag Concr Res 1981;33(114):48–60.

[16] Hassan KE, Cabrera JG, Maliehe RS. The effect of mineral admixtures on the properties of high-performance concrete. Cement Concr Compos 2000;22(4):267–71.

[17] Nilsen U, Sandberg P, Folliard K. Influence of mineral admixtures on the transition zone in concrete. In: Maso JC, editor. Proceeding of the RILEM International Conference, Toulouse. 1992. p. 65–70.

[18] Memon AH, Radin SS, Zain MFM, Trottier JF. Effects of mineral and chemical admixtures on high-strength concrete in seawater. Cement Concr Res 2002;32(3):373–7.

[19] Papadakis VG, Vayenas CG, Fardis MN. Physical and chemical characteristics affecting the durability of concrete. ACI Mater J 1991;8(2):186–96.

[20] Cao HT, Sirivivatnanon V. Corrosion of steel in concrete with and without silica fume. Cement Concr Res 1991;21(2/3):316–24.

[21] Matte V, Moranville M. Durability of reactive powder composites: influence of silica fume on the leaching properties of very low water binder pastes. Cement Concr Compos 1999;21(1):1–9.

[22] Bentz DP, Stutzman PE. Evolution of porosity and calcium hydroxide in laboratory concretes containing silica fume. Cement Concr Res 1994;24(6):1044–50.

[23] Yogendran V, Langan BW, Ward MA. Hydration of cement and silica fume paste. Cement Concr Res 1991;21(5):691–708.

[24] Larbi JÁ, Fraay ALA, Bijen JMJM. The chemistry of the pore fluid of silica fume-blended cement systems. Cement Concr Res 1990;20(4):506–16.

[25] Mangat PS, Molloy BT. Influence of PFA, slag and microsilica on chloride induced corrosion of reinforcement in concrete. Cement Concr Res 1991;21(5):819–34.

[26] Winslow DN, Cohen MD, Bentz DP, Snyder KA, Garboczi EJ. Percolation and pore structure in mortars and concrete. Cement Concr Res 1994;24(1):25–37.

[27] Scrivener KL, Nemati KM. The percolation of pore space in the cement paste/aggregate interfacial zone of concrete. Cement Concr Res 1996;26(1):35–40.

[28] Kobayashi K, Shuttoh K. Oxygen diffusivity of various cementitious materials. Cement Concr Res 1991;21(2/3):273–84.
[29] Raupach M, Gulikers J. Investigations on cathodic control of chloride-induced reinforcement corrosion. EUROCORR 1999, Aachen (on CD).
[30] Hughes DC. Pore structure and permeability of hardened cement paste. Mag Concr Res 1985;37(133):227–33.
[31] Allen AJ, Livingston RA. Relationship between differences in silica fume additives and fine-scale microstructural evolution in cement based materials. Adv Cement Based Mater 1998;8(3–4):118–31.
[32] Amaral ST, Müller IL. A RRDE study of the electrochemical behaviour of iron in solutions containing silicate and sulphate at pH 10–13. Corros Sci 1999;41(8):759–71.
[33] Sagüés AA, Pickering HW. Crevice effect on corrosion of steel in simulated concrete pore solution. Corrosion 2000;56(10):979–82.
[34] Nepomuceno AA, Bauer E, de Vasconcelos KL. Study of corrosion inhibitor of steel in concrete using polarization resistance (Rp), exposed to chloride environments. In: IV Congresso Iberoamericano de Patologia das Construções, VI Congresso de Controle de Qualidade, Anais, Porto Alegre, vol. 1. LEME/CPGEC, Dpto. de Eng. Civil, UFRGS, 1997. p. 161–8 [in Portuguese].
[35] Hou J, Chung DDL. Effect of admixtures in concrete on the corrosion resistance of steel reinforced concrete. Corros Sci 2000;42:1489–507.
[36] Al-Amoudi OSB. Durability of reinforced concrete in aggressive Sabkha environments. ACI Mater J 1995;92(3):236–45.